Hindawi
Shock and Vibration
Volume 2018, Article ID 3128268, 10 pages
https://doi.org/10.1155/2018/3128268

Research Article

A SHPB Experimental Study on Dynamic Mechanical Property of High-Damping Rubber

Xiudi Li,[1,2] **Huaiyuan Mao**,[1] **Ke Xu**,[1] **and Chaoyang Miao**[3]

[1]*Department of Military Facility, The Army Logistics University of PLA, Chongqing 401311, China*
[2]*Chongqing Key Laboratory of Geomechanics & Geoenvironment Protection, The Army Logistics University of PLA, Chongqing 401311, China*
[3]*No. 89800 Army Force of PLA, Beijing 100000, China*

Correspondence should be addressed to Huaiyuan Mao; maohuaiyuan@gmail.com

Received 23 January 2018; Revised 14 June 2018; Accepted 26 June 2018; Published 10 July 2018

Academic Editor: Stefano Sorace

A split Hopkinson pressure bar (SHPB) experiment was done to examine the feasibility and explosion resistance of high-damping rubber materials developed for use in the area of antiexplosion applications. Through the experiment, the dynamic mechanical properties of the high-damping rubber were determined. The existence of dynamic compressive stress-strain curves at various strain rates of the high-damping rubber have been confirmed from the SHPB experiment. The variation law of the dynamic compression performance with the strain rate is studied, and the energy absorption characteristics of high-damping rubber materials are analyzed. To study the microstructural changes of the high-damping rubber before and after impact, a scanning electron microscopy (SEM) test was done. The results indicated that the stress-strain curve and dynamic modulus of high-damping rubber has an obvious strain rate effect, and the strength and energy absorption ability of high-damping rubber material increases with an increase in the strain rate; the ideal energy absorption efficiency of high-damping rubber can reach 0.8 at a high strain rate and the ideal energy absorption efficiency is more than 0.5 in a wide deformation range; when compared with aluminum foam, the energy absorption effect for high-damping rubber is more apparent. In the event of a compressed deformation or the creation of holes, there may be a change in the main internal mechanism of the high buffering and energy absorption capacity of the high-damping rubber.

1. Abstract

In recent years, with the continuous occurrence of military conflicts, accidental explosions, and terrorist attacks, more emphasis has been directed towards the study of antiexplosion and the development of impact resistant materials; in addition, analyzing the structure of these components is a crucial area in civil engineering related to disaster prevention and safety projects. Presently, there are two main protection methods used for impact protection. First method is the use of thick traditional materials such as concrete, reinforced concrete, and masonry to reduce the impact of an explosion or exerted energy, while increasing the size of the structure to achieve a bigger explosion and impact energy absorption. The second option is the creation of composite explosion proof structure by combining high strength and energy consuming materials. Research reports have revealed that seeking for light, high-energy absorption, low cost, antiexplosion, and shock-resistance materials as well as the composite structure has become the main developmental focus in this field [1].

Aluminum foam, fiber-reinforced polymer, polyurea coatings, and high-damping rubber can be referred to as examples of materials that have the capacity to dissipate energy and be subsequently used for processes which involve explosion resistance. A. G. Evans [2] examined the capacity of aluminum foam to resist explosions. The experiment involved the use of empirical formulas to calculate the thickness of the aluminum foam needed to form a protective layer beneath a particular explosive load. G. Reyes Villanueva [3] carried out a high-speed impact response test on the composite materials with fiber-aluminum multilayer thin plates used as the panel and aluminum foam as a sandwich,

the study believed that the system has good energy absorption characteristics under high-speed impact. Hutchinson [4] proved that due to the fluid-structure interaction, in a water environment, the sandwich plates have a higher capacity than the monolithic plates to withstand higher water shocks, in situations where both structures have an equal mass and material; in addition, the optimal designs depend on the details of this interaction. Zahra S. Tabatabaei [5] carried out experimental testing and numerical simulation on ordinary reinforced concrete slabs and reinforced concrete slabs with a long carbon fiber. The outcome revealed that the inclusion of long carbon fiber caused a notable increase in the blast resistance of the concrete, subsequently; there was a lower degree of cracking as observed on the concrete panels. J. M. Pereira [6] proved that the CFRP strengthened steel structure could effectively reduce the stress around the crack. Dinan [7] proved by experiments that the thin film structure of a high elastic body can strengthen the flexural rigidity and resistibility of the wall. At the Mexico Polytechnic University [8] a smaller experiment was done by performing an equivalent explosion testing on the wall. During this experiment, the wall was sprayed with PAXCONTM. The experiment indicated that the antiexplosive coating on the wall could absorb a lot of energy to improve the explosion resistance of the wall.

Common rubber is a type of polymer viscoelastic material, which has good energy absorption characteristics. In the process of rubber deformation, great internal friction will be produced to absorb energy [9]. Zhang Wei [10] applied the enhanced Hopkinson experimental device while conducting this experimental study to evaluate the three types of common rubber materials which have varying proportions, the results showed that the strain rate effect of rubber is obvious, and the hardness of rubber is an important factor affecting the energy absorption. Research reports for Wang Bing's study [11] showed that the rubber material has a certain ability to resist explosion; however, there is a limited protection, while the explosion resistance is observed to be significantly higher due to the reinforcement of the rubber with the fiber material. Considering the composite target with rubber filled into honeycomb sandwich as the research object, Zhu Yi [12] regarded the rubber-filled honeycomb sandwich panel as the research object and used LS-DYNA to study the explosion resistance performance of the rubber-filled honeycomb sandwich composite panel under different cellular placement modes (horizontal and vertical honeycomb placement).

The high-damping rubber consists of natural rubber reinforced with fillers to increase the range of desired properties such as the strength and damping capacities. In recent years, high-damping rubber has been widely used in the industry field such as structure seismic, bridge damping, controlling mechanical or equipment resonance, and instrument damping [9]. S. L. Burtscher [13] performed a compression and shear test to evaluate the anisotropic high-damping bearings, which is a method for maximally improving the structure isolation of high-damping rubber laminated bearings to the structure. A. Dall'Asta [14] carried out experiments to test the performance of high-damping rubber at different strain rates, from the results; a nonlinear viscoelastic damage model was developed to account for the characteristics of rubber during cyclic loading. Yoshida Junji [15] established a three-dimensional finite element model of the high-damping rubber bearing and proposed deformable design formulas based on the simulation or experimental results. A. Dall'Asta [16] examined the consequences of the nonlinear features observed during the dynamic response regarding the single degree of freedom system in accordance with the high-damping rubber, subsequently generating a restoring force through which the response of earthquake input at varying intensities can be evaluated.

Figure 1: High-damping rubber sample.

The researches about high-damping rubber materials mainly focus on seismic-isolation of the support [17], and research efforts on dynamic material models of high-damping rubber have been scarce. To extensively study the feasibility of high-damping rubber materials which are used in the area of antiexplosion and shock resistance, the impact dynamic properties of high-damping rubber under different strain rates were determined through the split Hopkinson pressure bar experiment acknowledged in this paper. In addition, the analysis also evaluated the energy absorption efficiency of high-damping rubber and the differences observed in the impact resistance of aluminum foam. The research results provide the foundation for further research in the future regarding the application of high-damping rubber in the field of antiexplosion and impact resistance.

2. Test Method

2.1. High-Damping Rubber Material Sample. It has been determined that the process of stress wave propagation is limited by high-damping rubber samples. In order to reduce the stress in homogeneity of the sample's two ends in the experiment, the thickness of the rubber sample should be reduced to the least possible minimum [18]. The research [19] shows that when the ratio of sample length to sample radius $l/r = 0.875+0.540\varepsilon_{end}$, the inertia effect and the friction effect of the sample in the SHPB test are small, and ε_{end} is the final strain value of the sample. Figure 1 shows the high-damping

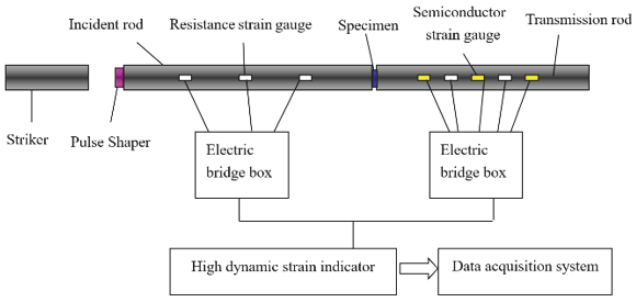

Figure 2: Diagram of the test device.

rubber which was processed to develop cylindrical specimens that had a thickness of 2mm and a diameter of 8mm.

2.2. Split Hopkinson Pressure Bar Device. The equipment selected for this impact compression test is a 14.5mm diameter aluminum SHPB test device. The striker, an incident rod, and transmission bar were all made from high strength aluminum; the lengths were 500mm, 1434mm, and 1495mm, respectively.

The three groups of resistance strain chips on the incident rod were positioned at 300mm, 600mm, and 900mm from the rubber sample. The three groups of semiconductor strain gauges on the transmission rod were observed to be at 300mm, 600mm, and 900mm from the sample. The resistance strain chips on the transmission rod were also determined to be at 450mm and 700mm from the sample and the contact surface of transmission rod. The appropriate strain gauges on the transmission rod were also selected based on how well they suit the experiment. For this process, the values of sensitivity coefficients obtained for the resistance strain gauge and the semiconductor strain gauge are 2.08 and 110, respectively. The diagram of the test device is shown in Figure 2.

2.3. Improvement Measures for Split Hopkinson Pressure Bar. The research reports indicated that [20] the conventional SHPB experiment with a soft specimen results in invalid data due to nonhomogeneous deformation during dynamic compression. Regarding the low wave impedance (the product of the material's longitudinal wave velocity and density) and low strength of the high-damping rubber materials against the traditional SHPB tests, the following areas were enhanced in this test:

(1) It is essential that the high-damping rubber sample fully meets the requirements for stress uniformity and the basic assumption of the SHPB [21]. This can be achieved by selecting a rubber sample of about 2mm. The shape of the loading pulse must be controlled to achieve a rise time that is longer than the stress equilibrating time in the specimen [20]. The application of an adhesive plaster before the incident bar can enhance the pulse loading wave form, subsequently reducing the rising edge of the incident wave form while increasing the time of stress equilibrium. A pulse shape technique which is part of a modified SHPB technique is found to be essential for rubber specimens being in dynamic stress equilibrium and to deform under a nearly constant strain rate [22].

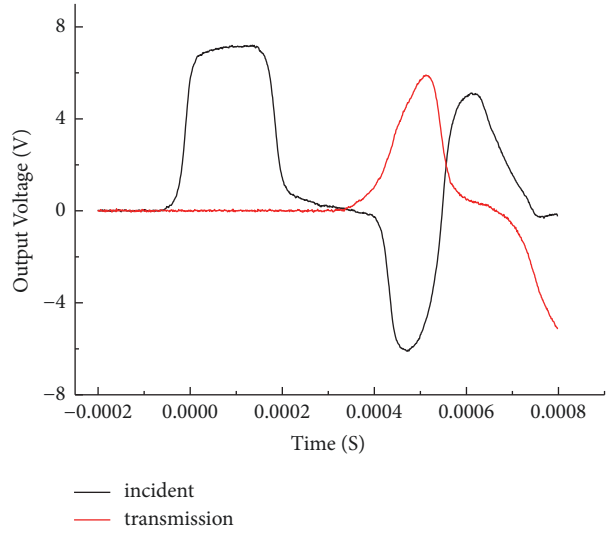

Figure 3: Typical waveforms at high strain rate.

(2) For weak transmission signal, in addition to using the aluminum rod with low material impedance, an alteration is done to change the method of measuring transmission signals. In this experiment, because the impedance of high-damping rubber sample is low and the transmission signal is small when the strain rate range is $\dot{\varepsilon} < 2000/s$, highly sensitive semiconductor strain gauges are used to collect transmission signals. At a higher strain rate, the transmission signal increases while a significant nonlinearity is observed in the semiconductor strain gauge (usually when $\varepsilon \geq 500\mu\varepsilon$, the nonlinearity features of the semiconductor strain gauge will be apparent), and the signal will exceed the range of the semiconductor instrument. Therefore, the transmission signal for the larger strain rate was determined by using the traditional resistance strain gauge. The illustration in Figure 3 shows the typical waves of incident and transmission waves which are measured at a high strain rate range while the transmission signal is measured with the resistance strain gauge.

(3) Since the traditional SHPB measurement technology is limited by the length of the compression rod, there is a limitation of maximum measurable strains in material testing applications [23]. It is difficult to discuss the large strain phenomenon of soft materials, especially when the strain rate is low, and the disadvantage is more obvious. So when the max strain was less than 45%, the evaluation of the mechanical properties of rubber materials was done by assessing two sets of incident and transmitted signals at different distances measured by a two-point strain gauge, and the mechanical performance data

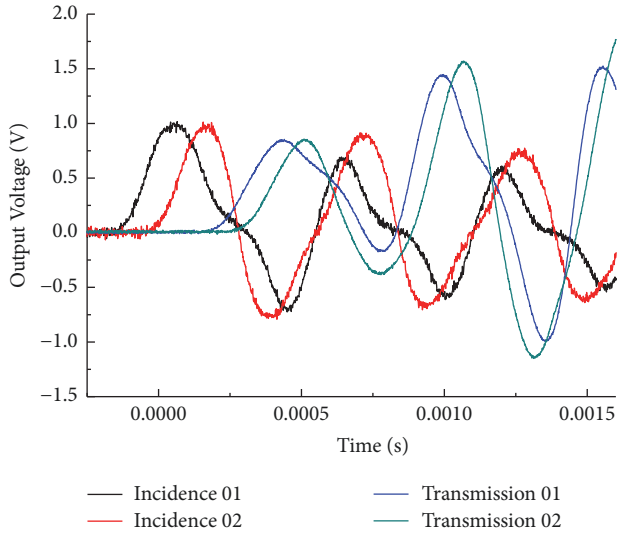

Figure 4: Typical waveforms obtained by two-point strain measurement.

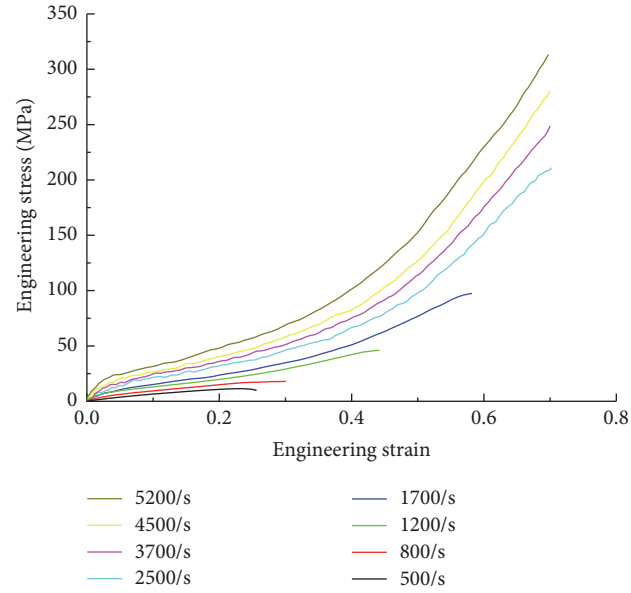

Figure 5: Engineering stress-strain curves of high-damping rubber material.

at a greater strain was obtained by using the waves separation technique. Figure 4 shows an illustration of the typical waveforms for two sets of the incident and transmitted waves, and the values were obtained from the two-point measurement used to evaluate the strain gauge; the transmission signal is measured by a semiconductor strain gauge. The distances between the incident strain gauge and the impact end of incident rod were 300mm and 900mm, respectively. In addition, the distances between the transmission strain gauge and the sample which is a transmission rod with a contact end face were found to be 300mm and 900mm, respectively.

3. Experimental Data Process

The impact compression tests were carried out while considering 8 different strain rates, which are 500/s, 800/s, 1200/s, 1700/s, 2500/s, 3700/s, 4500/s, and 5200/s, respectively. Regarding the high-damping rubber, the stress-strain curves obtained at the various strain rates are illustrated in Figure 5.

From the results, the measured maximum strain is less than 40% when the strain rates are 500/s and 800/s; hence a two-point strain gauge was used to measure and recalculate the stress-strain curve at large strain with the method of wave separation [24]. The resulting engineering stress-strain curves obtained are illustrated in Figure 6.

The two sets of stress-strain curves obtained from wave separation method were compared with other curves, and the final engineering stress-strain curve of the high-damping rubber under different strain rate is shown in Figure 7

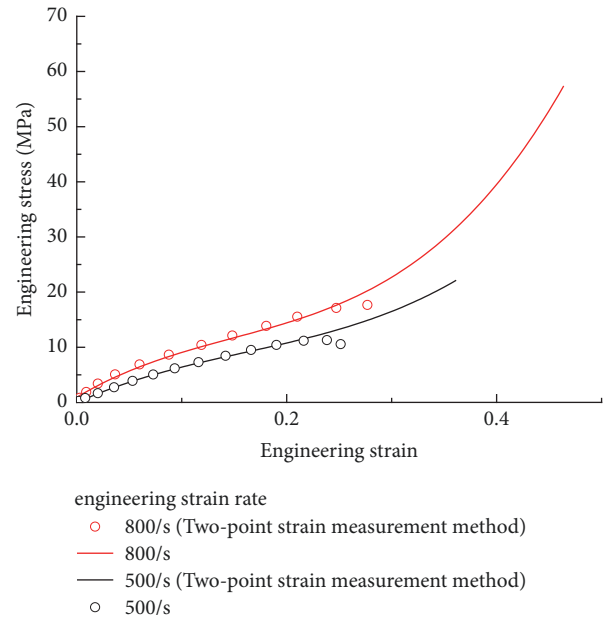

Figure 6: Comparison of engineering stress-strain curves obtained from conventional methods and wave separation method.

4. Experiment Results Analysis

4.1. Performance of Compressive Stress and Strain. Regarding Figure 7, the stress-strain curve of the high-damping rubber includes three stages which are as follows: elastic region, yielding region, and the densification region.

When the strain is less than 0.05, the stress-strain curve exhibits the features of a straight line. It can be assumed that the rubber at this time is in the elastic region. Therefore, the stress-strain ratio of $\varepsilon = 0.05$ was considered as the elastic modulus of the rubber, and the results are shown in Table 1. It is noteworthy to point out that the second stage of high-damping rubber shows a gradually upwarping trend, and the yield plateau is not very obvious. The stress of

Table 1: Initial elastic modulus under different strain rate.

Strain rate	5200/s	4500/s	3700/s	2500/s
E_0(MPa)	485.20	413.71	336.87	284.16
Strain rate	1700/s	1200/s	800/s	500/s
E_0(MPa)	141.75	81.45	80.22	63.61

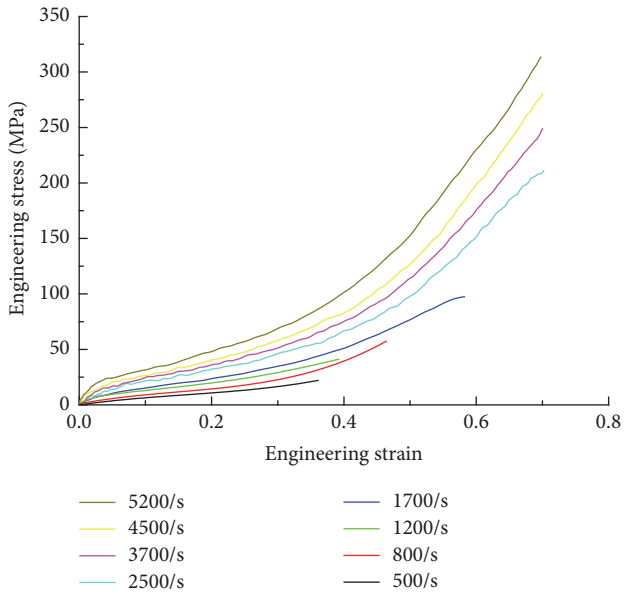

Figure 7: The final engineering stress-strain curves under different strain rates.

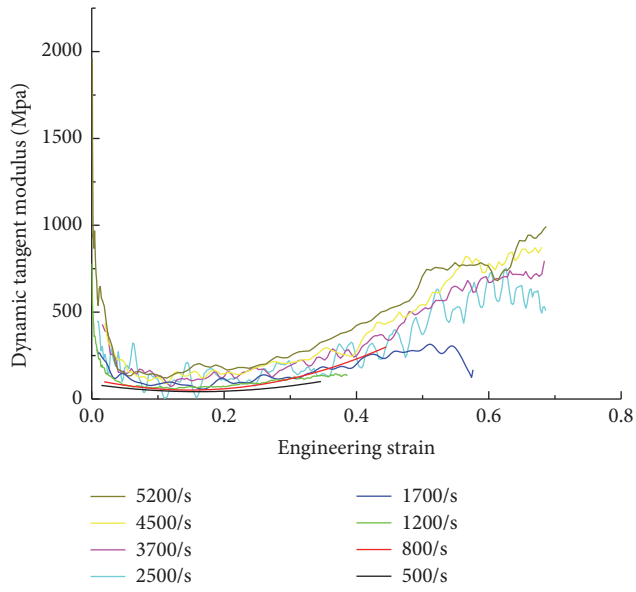

Figure 8: Dynamic modulus curve of high-damping rubber.

high-damping rubber at the yield stage rises gradually with increases in the strain. In the densification region, with the increase of the strain rate, the stress-strain curve of high-damping rubber material exhibits a concave feature, referred to as the hardening phenomenon, and it shows a crucial correlation with the strain rate. The integral area under the stress-strain curve increases; subsequently, there is a higher energy absorption of the material. The greater the strain rate, the greater the dynamic elastic modulus of the rubber. This is an indication that high-damping rubber is sensitive to shock waves, and it is adequate as an antiexplosion material and to achieve impact resistance.

According to the engineering stress-strain curves of high-damping rubber at different strain rates in Figure 7, high-damping rubber also showed an engineering dynamic modulus curve as depicted in Figure 8.

From Figure 8, in addition to the lack of data when ε is close to 0 by using the wave separation method at 500/s and 800/s, the illustrations that represent other dynamic modulus curves are observed to depict a sharp decline—remaining steady—steadily rising. It can be visually observed that, for the same strain, stress and dynamic modulus of rubber with high strain rate were greater than the value of rubber with low strain rate; in addition, the initial slope and peak dynamic modulus of rubber curve obviously change with the strain rate, rising with an increase in the average strain rate. It is observed that the dynamic features of rubber materials can be influenced by the impact load at different strain rates.

It is also apparent from Figure 8 that the values of dynamic modulus significantly drop when there is a change in the strain of high-damping rubber from 0 to 0.04. For example, when the strain rate is 5200/s, the dynamic modulus decreases from 1656MPa to 251Mpa, reducing by 85%. At the stage where the strain increases from 0.04 to 0.05, the dynamic modulus of each group experiences a minimal change, while the value remains stable. At the stage where the strain changes from 0.05 to 0.1, the dynamic modulus decreases gradually. When the strain reaches about 0.1, the dynamic modulus drops to its lowest value, before gradually rising. From the analysis of the entire stage, the following can be inferred:

(1) When $\varepsilon \leq 0.04$, the rubber just contacts the impact wave and the stress is very large. But it has not been able to deform yet, so the dynamic modulus is very large and gradually decreasing.

(2) When $0.04 \leq \varepsilon \leq 0.05$, the rubber is in an elastic state. When the strain reaches 0.05, the rubber begins to yield, so the dynamic modulus decreases gradually.

(3) When $0.1 \leq \varepsilon$, the rubber enters the densification region and the dynamic modulus increases gradually. This is in accordance with the stress-strain diagram in Figure 7.

4.2. Energy Absorption Analysis under Different Strain Rates. The main evaluation indexes of energy absorption performance are as follows.

(1) Energy Absorption Diagram of Materials. Maiti and Gibson proposed the method of energy absorption diagram [25], and the energy curve absorbed by the unit volume rubber could be got by the integral processing of the stress-strain curve from the test. That is to say, from the initial compression to the dense stage, the area under the stress-strain curve is Q, which represents the energy absorbed by the buffer volume of the unit volume during the compression to the dense stage. It characterizes the energy absorption capacity of the material.

The expression of Q is

$$Q = \int_0^{\varepsilon_i} \sigma d\varepsilon \tag{1}$$

where ε_i is the arbitrary strain.

(2) Energy Absorption Efficiency of Materials. Miltz [26] defined the expression of energy absorption efficiency E of materials:

$$E = \frac{\int_0^{\varepsilon_i} \sigma d\varepsilon}{\sigma_i} \tag{2}$$

where ε_i is the arbitrary strain and σ_i is the stress corresponding to the strain.

Formula (2) shows that the energy absorption efficiency of the material E is the ratio of the energy absorbed by the material to the corresponding stress when the material reaches a strain ε_i. When the energy absorption efficiency E of the material reaches the maximum value, it shows that the energy absorbing property of the cushion materials is the best at this stress and its dissipation capacity can be brought into full play.

(3) Ideal Energy Absorption Efficiency. Miltz [26] defined the expression of the ideal energy absorption efficiency I of the material:

$$I = \frac{\int_0^{\varepsilon_i} \sigma d\varepsilon}{(\sigma_i \times \varepsilon_i)} = \frac{E}{\varepsilon_i} = \frac{Q}{(\varepsilon_i \times \sigma_i)} \tag{3}$$

where the meanings of ε_i and σ_i are the same as above.

It can be observed in formula (3) that the ideal energy absorption efficiency I of the material represents the ratio of energy absorbed by the real rubber and ideal rubber samples at the same strain level.

The research shows that [27] the curve of ideal energy absorption efficiency of materials should be chosen to compare the energy absorption properties of different materials. In the case of a specific material, the curve of energy absorption efficiency of the material should be selected as a means of identifying the optimum working rate of its energy absorption. The curves of energy absorption, energy absorption efficiency, and ideal energy absorption efficiency of high-damping rubber were calculated respectively, as shown in Figures 9–11.

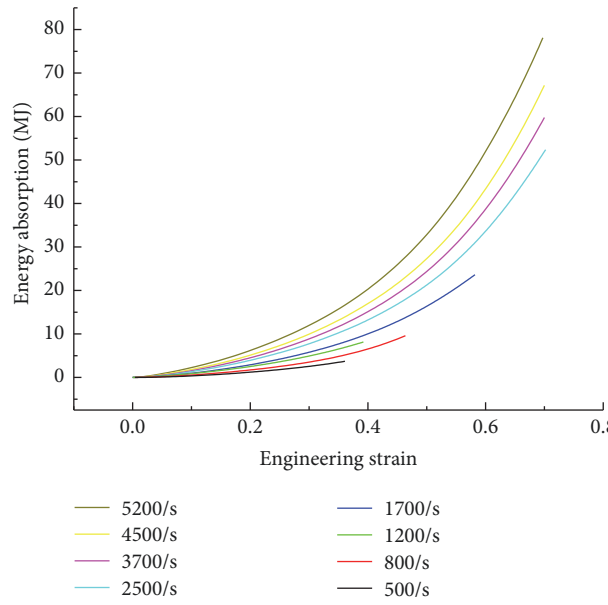

Figure 9: Energy absorption curves of high-damping rubber.

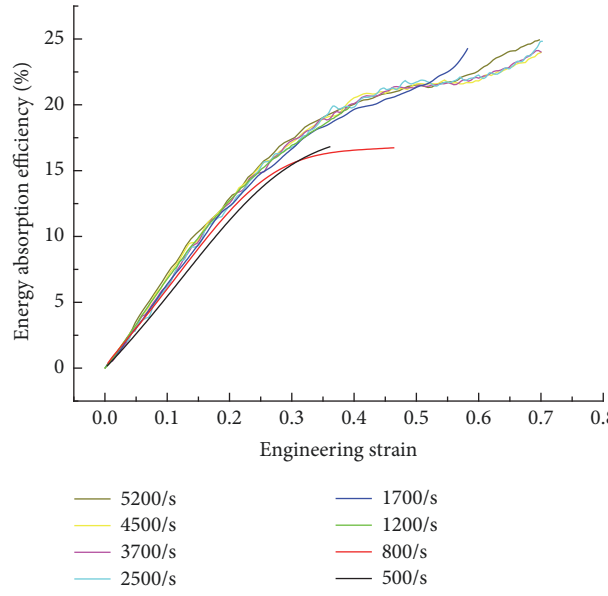

Figure 10: Curves of energy absorption efficiency of high-damping rubber.

From Figures 9 and 10, it can be seen that the energy absorption of high-damping rubber rises with an increase in the strain. A higher strain rate causes an increase in the energy absorption capacity. The energy absorption efficiency increases quickly at first with the increase in strain and then increases slowly. Regarding the small strain range, there is little difference in energy absorption efficiency at a different strain rate. It can be affirmed that at a higher strain rate there will be greater energy absorption efficiency.

From Figure 11, it is observed that the ideal energy absorption efficiency of the high-damping rubber is sustained at a high level during the early stages of deformation (when

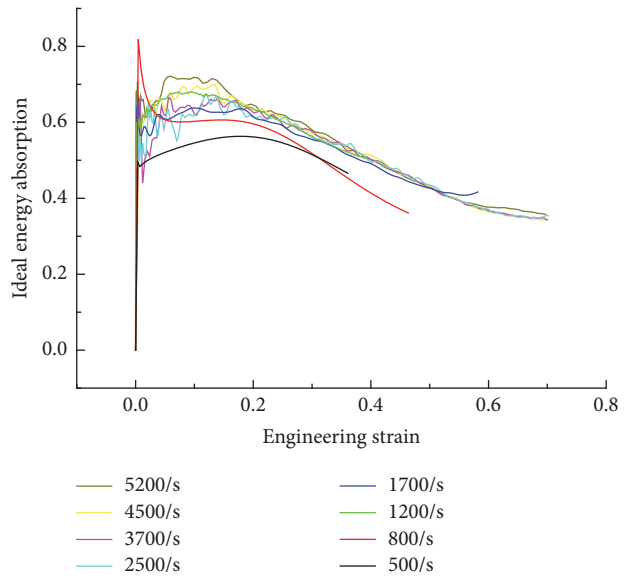

Figure 11: Curves of ideal energy absorption efficiency of high-damping rubber.

the strain is less than 0.2). With the further increase of the strain (at a value greater than 0.2), the ideal energy absorption efficiency of the high-damping rubber reduces to about 0.4. Within a wider strain range (when the strain is less than 0.3), the ideal energy absorption efficiency of the high-damping rubber is consistently above 0.5. This is an indication that high-damping rubber can be regarded as a reliable cushioning energy absorbing material.

4.3. Comparative Analysis of Shock Resistance of High-Damping Rubber and Aluminum Foam. Aluminum foam was widely regarded as a buffering and energy absorbing material and has been frequently used in different studies to resist impact. Tian Jie [28] studied the dynamic mechanical properties of four kinds of aluminum foam materials by performing a split Hopkinson pressure bar test and obtained the stress-strain curves at different strain rates. Wang et al. [29] evaluated the dynamic mechanical properties of aluminum foam materials by performing a SHPB test and obtained the stress-strain relation curve of foamed aluminum under the condition of a large strain rate. We selected the stress-strain curve of industrial pure aluminum foam at a strain rate of 2000/s (as shown in Figure 12) to be used in comparison with the value of high-damping rubber. The absence of an apparent difference between energy absorption efficiency and the ideal energy absorption efficiency when there is a change in the strain rate makes it possible for the energy absorption efficiency and ideal energy absorption efficiency at strain rate of 1700/s and 2500/s to be used for approximately determining the energy absorption efficiency and ideal energy absorption efficiency of high-damping rubber at strain rate of 2000/s. From Figures 7 and 12, it can be seen that, with the increase of strain, a similar trend can be observed for the stress development of aluminum foam and

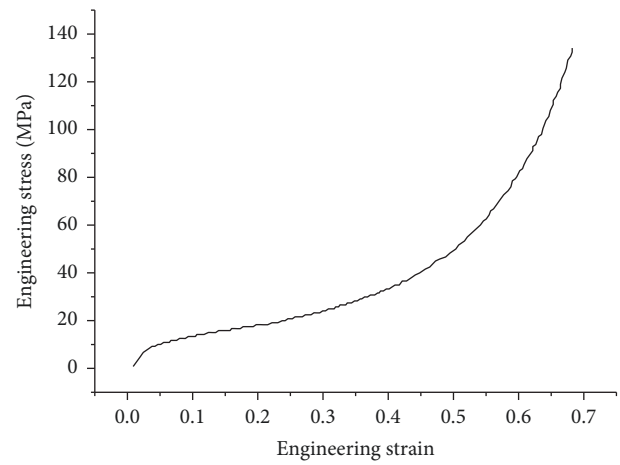

Figure 12: Stress-strain curve of industrial pure aluminum foam.

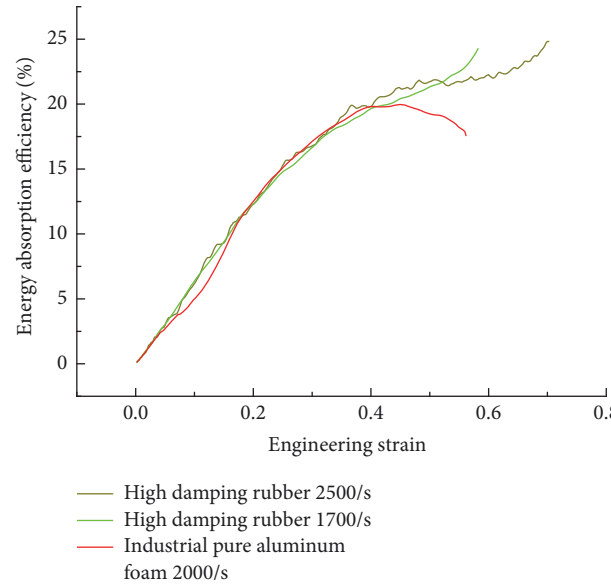

Figure 13: Comparison of curve of energy absorption efficiency.

the high-damping rubber; however, the strength of the high-damping rubber is significantly greater.

Energy absorption efficiency and ideal curve of energy absorption efficiency of aluminum foam were calculated, respectively, by using formulas (2) and (3). For the convenience of comparison, the correlation curves of the high-damping rubber at the strain rate of 2500/s and 1700/s are given together, as shown in Figures 13 and 14.

Figures 13 and 14 show the trend where the increase of strain, the energy absorption efficiency, and the ideal energy absorption efficiency of aluminum foam increases rapidly at first then the rate of increase slows down, and the peak values are about 20% and 0.6 respectively; compared with aluminum foam, the energy absorption efficiency of high-damping rubber shows a little difference when the strain is less than 0.4. However, when the strain is greater than 0.4, the energy absorption efficiency of aluminum foam

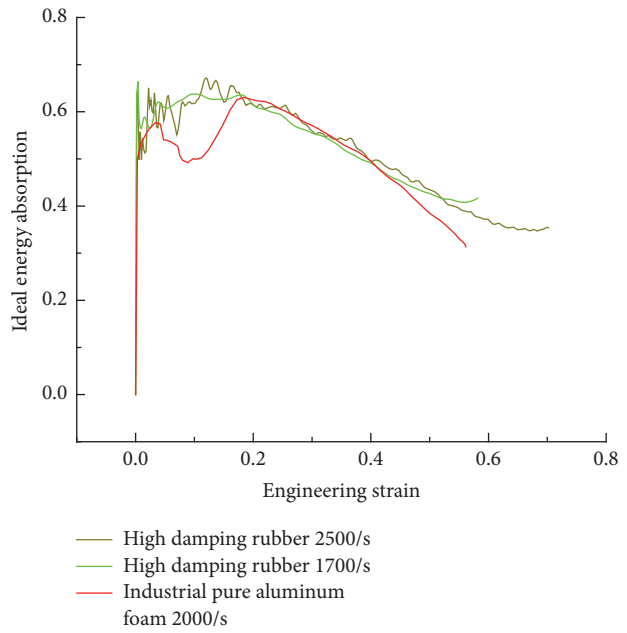

Figure 14: Comparison of ideal curve of energy absorption efficiency.

Figure 15: SEM test.

decreases while the energy absorption efficiency of high-damping rubber continues to increase. The ideal energy absorption efficiency of high-damping rubber attains its peak at the initial stage of deformation, subsequently; the relatively high level is sustained at a particular strain range. Furthermore, in the case of the aluminum foam a drop is first witnessed before a rise to the highest value when strain is less than 0.2. The ideal energy absorption efficiency of high-damping rubber decays slower than aluminum foam when the strain is greater than 0.2, which means that high-damping rubber can absorb more energy than aluminum foam under the same conditions. Comparing high-damping rubber with aluminum foam reveals that the high-damping rubber has a more prominent energy absorption energy effect potentially due to the unique damping mechanism of the high-damping rubber.

5. Microstructure Analysis of High-Damping Rubber

5.1. SEM Test of High-Damping Rubber. A scanning electron microscopy (SEM) test was carried out for the high-damping rubber before and after the impact of the split Hopkinson pressure bar test. The aim was to observe microscopic features within the material. SEM is as shown in Figure 15.

There are two experimental samples, one is a high-damping rubber sample before impact and the other is a high-damping rubber sample after the impact of 20.58m/s. It can be observed that the sample after the impact exhibited signs of plastic deformation. The experimental samples can be viewed in Figure 16.

5.2. Microanalysis of Energy Absorption Characteristics of High-Damping Rubber. Figure 17 shows a magnified illustration that represents the sample at a magnification of 500 times and 1,000 times, displaying the pre- and postimpact effects.

As seen in Figure 17, there existed a large number of dispersed independent holes in the high-damping rubber specimens before the impact. After the impact, some high-damping rubbers which have closer spaced holes were torn. Those spaced holes were merged to form larger holes; however, there were obvious microcracks near the holes. The results of the SEM test indicated that compression of high-damping rubber and expansion of internal holes should result in high buffering and absorption capacity under explosion shock impact. Therefore, it can be affirmed that high-damping rubber has good prospects for explosion resistance.

6. Conclusions

(1) Stress-strain relation curves and dynamic modulus of high-damping rubber at different strain rates were obtained by improving the split Hopkinson pressure bar test. From the analysis, it was observed that the stress-strain curve and dynamic elastic modulus of high-damping rubber undergo a significant strain rate effect. It forms the foundation for further research on antiexplosion and impact resistance of high-damping rubber materials.

(2) The calculation indicates that the ideal energy absorption efficiency of high-damping rubber can reach the value 0.8 at high strain rates. In a wide deformation range, the ideal energy absorption efficiency is greater than 0.5, which indicates that high-damping rubber can be regarded as a good energy absorption material.

(3) Compared with aluminum foam, high-damping rubber has a more pronounced energy absorption energy effect. When compared with aluminum foam, the energy absorption efficiency and the ideal energy absorption efficiency of high-damping rubber per

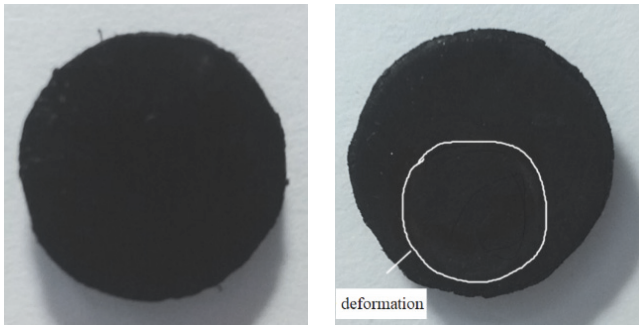

(a) Before the impact (b) After the impact

Figure 16: High-damping rubber samples before and after impact.

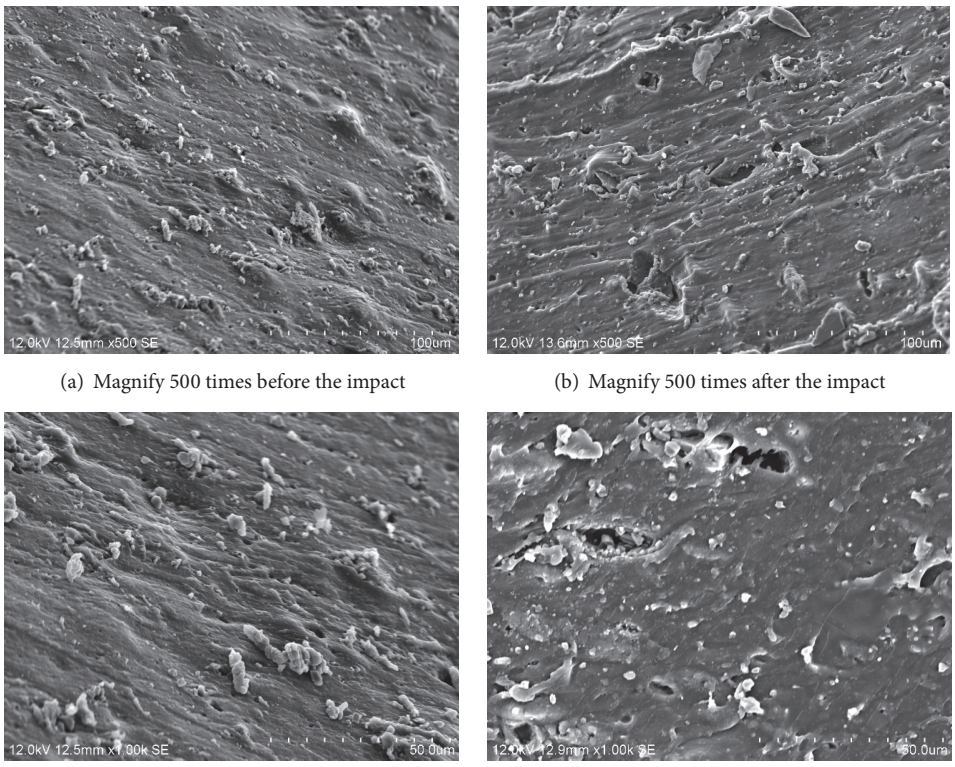

(a) Magnify 500 times before the impact (b) Magnify 500 times after the impact

(c) Magnify 1000 times before the impact (d) Magnify 1000 times after the impact

Figure 17: Microstructure of sample before and after impact.

unit volume are higher; this is an indication that high-damping rubber has the capacity to absorb more energy than aluminum foam in similar conditions.

(4) Regarding the scanning electron microscopy (SEM) experiment, it is observed that the compression deformation and the high number of holes tearing internally under impact may form the basis for the buffering and energy absorption capacity of the high-damping rubber.

Data Availability

The data used to support the findings of this study are available from the corresponding author upon request.

Conflicts of Interest

The authors confirm that this paper's content has no conflicts of interest.

Acknowledgments

This study was sponsored by the graduate innovative project grant of the Army Logistics University of PLA and the National Natural Science Foundation of China [Grant no. 51378496] and the National Ministries Research Projects [Grant no. CY213J009].

References

[1] Y. X. Wang, Y. X. Gu, and M. Sun, "Blast-resistant calculation of compound structure with porous material under impact Load," *Acta Armamentarii*, vol. 27, no. 2, pp. 375–379, 2006 (Chinese).

[2] A. G. Evans, J. W. Hutchinson, and M. F. Ashby, "Multifunctionality of cellular metal systems," *Progress in Materials Science*, vol. 43, no. 3, pp. 171–221, 1998.

[3] G. R. Villanueva and W. J. Cantwell, "The high velocity impact response of composite and FML reinforced sandwich structures," *Composites Science and Technology*, vol. 64, no. 1, pp. 35–54, 2004.

[4] J. W. Hutchinson and Z. Y. Xue, "Metal sandwich plates optimized for pressure impulses," *International Journal of Mechanical Sciences*, vol. 47, no. 4-5, pp. 545–569, 2005.

[5] Z. S. Tabatabaei, J. S. Volz, J. Baird, B. P. Gliha, and D. I. Keener, "Experimental and numerical analyses of long carbon fiber reinforced concrete panels exposed to blast loading," *International Journal of Impact Engineering*, vol. 57, pp. 70–80, 2013.

[6] J. M. Pereira, H. Ghasemnejad, J. X. Wen, and V. H. Y. Tam, "Blast response of cracked steel box structures repaired with carbon fibre-reinforced polymer composite patch," *Materials and Corrosion*, vol. 32, no. 5, pp. 3092–3098, 2011.

[7] R. J. Dinan, J. W. Fisher, I. Michael et al., "Failure mechanisms in unreinforced concrete masonry walls retrofitted with polymer coatings," in *Proceedings of the The 1th International Symposium on Interaction of the Effects of Munitions with Structures*, vol. 12, pp. 5–9, 2003.

[8] J. S. Davidson, J. W. Fisher, M. I. Mammons, J. R. Porter, and R. J. Dinan, "Failure mechanisms of polymer-reinforced concrete masonry walls subjected to blast," *Journal of Structural Engineering*, vol. 131, no. 8, pp. 1194–1205, 2005.

[9] Q. M. Qin, "High damping rubber engineering applications," *Journal of Vibration and Shock*, vol. 4, pp. 36–41, 1993.

[10] W. Zhang, P. F. Zheng, C. Liu et al., "Energy absorption ratio of rubber material under dynamic impact load," *Ordnance Material Science and Engineering*, vol. 35, no. 5, pp. 19–21, 2012 (Chinese).

[11] B. Wang, Y. Long, and H. Y. Ma, "Energy absorption ratio of rubber material under dynamic impact load," *Explosive Materials*, vol. 30, no. 1, pp. 37–40, 2010.

[12] Y. Zhu, *Explosion Resistance of Rubber Filled Honeycomb Sandwich Composite Structures*, Nanjing University of Science and Technology, Nanjing, China, 2014.

[13] S. L. Burtscher and A. Dorfmann, "Compression and shear tests of anisotropic high damping rubber bearings," *Engineering Structures*, vol. 26, no. 13, pp. 1979–1991, 2004.

[14] A. Dall'Asta and L. Ragni, "Experimental tests and analytical model of high damping rubber dissipating devices," *Engineering Structures*, vol. 28, no. 13, pp. 1874–1884, 2006.

[15] J. Yoshida, M. Abe, Y. Fujino, and H. Watanabe, "Three-dimensional finite-element analysis of high damping rubber bearings," *Journal of Engineering Mechanics*, vol. 130, no. 5, pp. 607–620, 2004.

[16] A. Dall'Asta and L. Ragni, "Nonlinear behavior of dynamic systems with high damping rubber devices," *Engineering Structures*, vol. 30, no. 12, pp. 3610–3618, 2008.

[17] A. Dall'Asta, L. Dezi, R. Giacchetti et al., "Dynamic response of composite frames with rubber-based dissipating devices: experimental tests," in *Proceedings of the Fourth International Conference on Advances in Steel Structures*, pp. 741–746, Shanghai, China, 2005.

[18] W. Chen and B. Song, "One-Dimensional Dynamic Compressive Behavior of EPDM Rubber," *Journal of Engineering Materials Technology*, vol. 125, no. 3, pp. 294–301, 2003.

[19] J. L. Tao, Y. Z. Chen, C. T. Tian et al., "Analysis of the inertial effect of the cylindrical specimen in SHPB system," *Acta Mechanica Solida Sinica*, vol. 26, no. 1, pp. 107–110, 2005 (Chinese).

[20] W. Chen, F. Lu, D. J. Frew, and M. J. Forrestal, "Dynamic Compression Testing of Soft Materials," *Journal of Applied Mechanics*, vol. 69, no. 3, pp. 214–223, 2002.

[21] O. S. Lee, J. W. Lee, and S. H. Kim, "Dynamic deformation behavior of rubber(NR/NBR) under high strain rate compressive loading," in *Proceedings of the Asian Pacific Conference on Fracture and Strength*, vol. 10, pp. 172–177, 2005.

[22] B. Song and W. Chen, "Dynamic stress equilibration in split Hopkinson pressure bar tests on soft materials," *Experimental Mechanics*, vol. 44, no. 3, pp. 300–312, 2004.

[23] H. Zhao and G. Gary, "A new method for the separation of waves. Application to the SHPB technique for an unlimited duration of measurement," *Journal of the Mechanics and Physics of Solids*, vol. 45, no. 7, pp. 1185–1202, 1997.

[24] X. T. Wu, S. S. Hu, and R. F. Zhang, "Application of two points strain measurement to the SHPB technique," *Explosion and Shock Waves*, vol. 23, no. 4, pp. 309–312, 2003 (Chinese).

[25] S. K. Maiti, L. J. Gibson, and M. F. Ashby, "Deformation and energy absorption diagrams for cellular solids," *Acta Metallurgica et Materialia*, vol. 32, no. 11, pp. 1963–1975, 1984.

[26] J. Miltz and G. Gruenbaum, "Evaluation of cushioning properties of plastic foams from compressive measurements," *Polymer Engineering & Science*, vol. 21, no. 15, pp. 1010–1014, 1981.

[27] F. Zeng, Y. Pan, and S. S. Hu, "Evaluation of cushioning properties and energy-absorption capability of foam aluminium," *Combustion, Explosion, and Shock Waves*, vol. 4, pp. 358–362, 2002 (Chinese).

[28] J. Tian, *The Shock Wave Attenuation and Anti-Detonation Property of Aluminum Foam*, University of Science and Technology of China, Hefei, China, 2006.

[29] Y.-G. Wang, S.-S. Hu, and L.-L. Wang, "Shock attenuation in aluminum foams under explosion loading," *Baozha Yu Chongji/Explosion and Shock Waves*, vol. 23, no. 6, pp. 516–522, 2003 (Chinese).